Available online at www.sciencedirect.com
ScienceDirect
International Journal of Mass Spectrometry 255–256 (2006) 76–85
International Journal of Mass Spectrometry
www.elsevier.com/locate/ijms

The kinetics of the decompositions of the proton bound dimers of 1,4-dimethylpyridine and dimethyl methylphosphonate from atmospheric pressure ion mobility spectra

R.G. Ewing [a,*], G.A. Eiceman [b], C.S. Harden [c], J.A. Stone [d]

[a] *Chemistry Department, New Mexico Tech., Socorro, NM 87801, USA*
[b] *Department of Chemistry and Biochemistry, New Mexico State University, Las Cruces, NM 88003, USA*
[c] *U.S. Army Edgewood Chemical Biological Center, Aberdeen Proving Ground, MD 21010-5423, USA*
[d] *Department of Chemistry, Queen's University, Kingston, Ont., Canada K7L 3N6*

Received 27 September 2005; received in revised form 12 April 2006; accepted 13 April 2006
Available online 5 June 2006

Abstract

The rate constants for the dissociations, $A_2H^+ \rightarrow AH^+ + A$, of the symmetrical proton bound dimers of 2,4-dimethylpyridine and dimethyl methylphosphonate have been determined using an ion mobility spectrometer operating with air as drift gas at ambient pressure. Reaction time was varied by varying the drift electric field. The rate constants were derived from the mobility spectra by determining the rate at which ions decomposed in the drift region. Arrhenius plots with a drift gas containing water vapor at 5 ppm_v gave the following activation energies and pre-exponential factors: 2,4-dimethylpyridine, 94 ± 2 kJ mol^{-1}, $\log A$ (s^{-1}) $= 15.9 \pm 0.4$; dimethyl methylphosphonate, 127 ± 3 kJ mol^{-1}, $\log A$ (s^{-1}) $= 15.6 \pm 0.3$. The enthalpy changes for the decompositions calculated from the activation energies are in accord with literature values for symmetrical proton bound dimers of oxygen and nitrogen bases. The results for dimethyl methylphosphonate were obtained over the temperature range 478–497 K and are practically independent of water concentration (5–2000 ppm_v). The activation energy for 2,4-dimethylpyridine, obtained over the temperature range 340–359 K, decreased to 31 kJ mol^{-1} in the presence of 2.0×10^3 ppm_v of water. At the low temperature, a displacement reaction involving water may account for the decrease. The reduced mobilities of the protonated molecules and the proton bound dimers have been determined over a wide temperature range. While the values for the dimers are essentially independent of the water concentration in the drift gas, those of the protonated molecules show a strong dependence.

Keywords: Proton bound dimers; Ion mobility; Dissociation kinetics

1. Introduction

The bond strengths of the adducts formed by ions and neutral molecules have been investigated by many methods [1,2]. Measurement of equilibrium constants, K, for reactions $A^+ + B = AB^+$ lead to the determination of reaction standard free energies since $\Delta G^\circ = -RT \ln K$. The enthalpy of binding is then obtained from the expression $\Delta G^\circ = \Delta H^\circ - T\Delta S^\circ$, provided that a value for ΔS° can be obtained or calculated. Since ion–molecule associations are always exothermic, low pressure techniques using ion cyclotron resonance and ion trap instruments present difficulties because the limited lifetimes of the nascent complexes favor dissociation prior to collisional stabilization. Relative bond enthalpies may be estimated using these techniques from the free energy changes for switching reactions [3] but since the instruments are usually operated at ambient temperature, ΔS° must be calculated or estimated. Pulsed electron beam high pressure mass spectrometry (PHPMS) provides a means of experimentally determining both ΔH° and ΔS° because it often allows the measurement of equilibrium constants over a range of temperatures [4]. This technique also has the advantage that, as a consequence of multiple collisions with buffer gas at 4–10 Torr, all the participants of the equilibrium reactions are thermalized at known temperatures. One drawback of HPMS is that in order to attain equilibrium within the milliseconds timescale of the instrument, a known pressure of

* Corresponding author. Tel.: +1 505 835 6948; fax: +1 505 835 5364.
E-mail address: ewing@nmt.edu (R.G. Ewing).

1387-3806/$ – see front matter © 2006 Elsevier B.V. All rights reserved.
doi:10.1016/j.ijms.2006.04.003

the order of a milliTorr or more of the neutral molecule, B, is required in the ion source. For solids and liquids with very low vapor pressures, such a high pressure may be impossible to achieve, even at temperatures of 600 K or higher.

The fact that all association reactions are exothermic means that all the reverse dissociation reactions are endothermic. The strength of ion-molecule associations may then be obtained from measurement of the energies required for such dissociations. Kinetic energy dependent guided ion beam mass spectrometry experiments in which threshold dissociation energies are measured yield such data, after correcting for the spread in energies of the incident ions [5]. So far, these experiments have been limited to fairly small systems. The kinetic method [6] has been used to determine the relative enthalpies of binding of a wide variety of complexes, especially proton bound systems. The method is simple but the temperature associated with the dissociating ions remains an open question [6,7]. Rate constants for the dissociation of ion–molecule complexes measured under truly thermal conditions over a range of temperatures would yield activation energies directly via the Arrhenius equation, $\ln k = \ln A - E_a/RT$. In order to accomplish this, the adducts must first be formed in a suitable manner, the neutral molecule participants must then be removed so that the dissociation of the ion–molecule adduct can be followed as a function of time. To be assured that reaction takes place under thermal conditions, the dissociation must occur on a time-scale appropriate to the rate constant in an inert buffer gas with a sufficient collision frequency to ensure a continuing Boltzmann distribution of energies. In this paper, we report the use of the ion mobility spectrometer to accomplish this task. The advantages of the instrument are its operation at a pressure of one atmosphere and its operating temperature range of ambient to more than 500 K. In the usual mode of operation, ion drift times are of the order of milliseconds so that dissociation reactions with first-order rate constants of the order of $10^2\ s^{-1}$ may be observed. In these first experiments, the main focus has been on the dissociation of symmetrical proton bound dimers, $AHA^+ \rightarrow AH^+ + A$, where A is 2,4-dimethypyridine or dimethyl-methylphosphonate.

2. Experimental

The instrument used is an ion mobility spectrometer interfaced to a triple quadrupole mass spectrometer (Model MMS 160, PCP Inc., West Palm Beach, FL). The mobility spectrometer is contained in a stainless steel housing with vacuum flanges to prevent room contaminants from entering the system. Band heaters allow an operable temperature range of ambient to 530 K. The entire system is enclosed in an insulated housing to maintain a uniform temperature. The drift tube, 15 cm in length from the ion repeller to the ion collector, is composed of a series of stainless steel rings isolated electrically from each other by sapphire balls. The drift tube is separated into three 5 cm sections by two shutter assemblies. The first section, the ionization region, has an internal diameter of 1.41 cm and contains a ^{63}Ni ionization source. The remaining 10 cm drift region has an internal diameter of 4.25 cm. An aperture grid, located immediately in front of the detector plate, has a diameter of 3.18 cm. This grid is used to electrically shield the ion collector from capacitive coupling to the shutter grid drive signals. The ion collector is a 4.8 cm diameter stainless steel plate electrically isolated and shielded. At its center is a 0.6 cm hole to allow a fraction of the ions to pass towards the inlet of the mass spectrometer. Directly behind the ion collector is a plate sealed to a vacuum flange containing a 100 μm diameter orifice. This flange is connected to a small region containing ion lenses that is mechanically pumped to approximately 0.3 Torr. The opposite end of this region contains a skimmer cone with a 1.3 mm aperture leading to the mass spectrometer. The mass spectrometer housing is pumped by two $500\ L\ s^{-1}$ turbomolecular pumps. The front region is maintained at approximately 9×10^{-5} Torr while the rear region, containing an ion-counting multiplier, is at about 9×10^{-6} Torr.

A uniform electric field is established within the tube by means of a voltage divider connected to the individual ring electrodes and grounded at the ion collector end. By changing the potential applied to the source end over the range +4500 to +1500 V, the electric field strength is variable from 300 to $100\ V\ cm^{-1}$. Data collection and instrument control were performed using a PC operating with MS Dos Version 6.00.

Mobility spectra were obtained by pulsing one of the ion shutters while monitoring the ion intensity at the detector plate as a function of time. Mass spectra were recorded as a function of drift time in two ways: (a) by collecting all ions and (b) by monitoring a single ion. All mobility and mass spectra were obtained by accumulating signal from 1000 shutter pulses.

The clean dry air supplied to the instrument was generated using a pure air generator (737 Series Pure Air Generator, Aadco, Cleves, OH). The moisture content was maintained at approximately 5 ppm_v unless otherwise noted and was measured using a moisture meter (Panametrics Moisture Image Series I, Waltham, MA). The flow was split into two streams, the sample carrier gas, and the drift gas. The carrier gas flow was maintained at about $100\ mL\ min^{-1}$ and was used to introduce the sample into the ionization region. The drift gas flow, maintained at approximately $500\ mL\ min^{-1}$, was introduced at the detector end of the drift region and moved counter to ion drift to minimize the entrance of analyte neutrals to the drift region. The combined gas flows exited the drift tube in the ionization region just prior to the first ion shutter. A thermocouple in the gas exit port monitored the temperature of the atmospheric pressure gas. In experiments designed to study the effect of moisture, part of the gas stream was bubbled through water and then combined with the dry air. The ratio of the dry air to humidified air was adjusted to achieve the desired moisture content.

The two chemicals used in these studies, 2,4-dimethyl pyridine (DMP) and dimethyl methylphosphonate (DMMP) (Aldrich Chemical Co., Milwaukee, MN) were contained in Teflon permeation tubes situated in a gas generator (570C Precision Gas Standards Generator, Kin-Tek Laboratories Inc., Texas City, TX). The chamber containing the permeation tube was held at a constant temperature and a fraction of the sample stream passing through it was combined with a dilution flow and $100\ cm^3\ min^{-1}$ of this combination was used as the carrier gas.

The sample concentration was adjusted by varying both temperature and split flow ratios. The amount of sample introduced was slowly increased while monitoring the mobility spectrum until the required concentration was attained. The system was then allowed to equilibrate overnight before any measurements were made. Although, knowledge of the actual concentration was not important, based upon prior work with these chemicals the estimated concentration in the ionization region was approximately 0.5–1.0 ppm_v.

3. Results

The ion mobility spectrum, obtained with only air containing ~5 ppm_v of water present throughout the instrument, showed a single, dominant peak, the reactant ion peak (RIP). Mass spectrometry identified this as the hydrated proton, $(H_2O)_nH^+$, where n had a range of values that depended on the temperature. At ~500 K, the ions with $n = 2$ and 3 predominated while at ambient temperature the range shifted to $n = 3$ and 4. When DMP or DMMP was introduced to the ion source held at a fixed temperature the RIP decreased in intensity as $(H_2O)_nH^+$ transferred a proton to the base and one or two peaks representative of the protonated base appeared at longer time than the RIP. The first new peak to appear at low base concentration was due to the protonated molecule and the second was due to the proton bound dimer. No proton bound trimer was observed. Such behavior has been described in detail in a previous paper from this laboratory for a number of alcohols, ketones, ethers, and amines [8].

Fig. 1 shows data obtained with the mobility spectrometer at a temperature of 353 K when DMP was introduced to the ion source at a sufficient concentration that the RIP and peaks due to $(DMP)H^+$ and $(DMP)_2H^+$ were present. Fig. 1a shows spectrum recorded at the mobility spectrometer detector plate when the 10 cm drift length was used. The total ion intensity measured by the mass spectrometer detector is shown in Fig. 1b. The 0.83 ms increase in the measured time for all peaks compared with those in Fig. 1a is due to the extra distance traveled by the ions from the detector plate to the mass spectrometer ion multiplier. The first peak in both spectra is the RIP, $(H_2O)_nH^+$. Fig. 1c shows the single ion spectrum for m/z 108 that identifies the central mobility spectrum peak 2 as $(DMP)H^+$ and similarly Fig. 1d identifies peak 3 as $(DMP)_2H^+$ at m/z 215. It is to be noted that in both Fig. 1a and 1b the signal does not return to the baseline between the $(DMP)H^+$ and $(DMP)_2H^+$ peaks. Fig. 1c shows that the ion associated with this phenomenon is $(DMP)H^+$. These ions, which have a greater drift time than the normal $(DMP)H^+$ ions comprising peak 2, must have traveled part of the drift distance as different, more slow-moving ions. They are due to ions that commenced life at the shutter as $(DMP)_2H^+$ and subsequently dissociated to $(DMP)H^+$ in the drift region (Eq (1)) before arriving at the detector.

$$(DMP)_2H^+ \rightarrow (DMP)H^+ + DMP \quad (1)$$

The $(DMP)_2H^+$ ions have their highest concentration in the drift region at the shutter and the concentration declines with time according to the first-order expression of Eq. (2). The intensity of the decomposing ions on the drift time scale is therefore, as observed in Fig. 1c, highest right next to the $(DMP)H^+$ peak and declining towards the $(DMP)_2H^+$ peak.

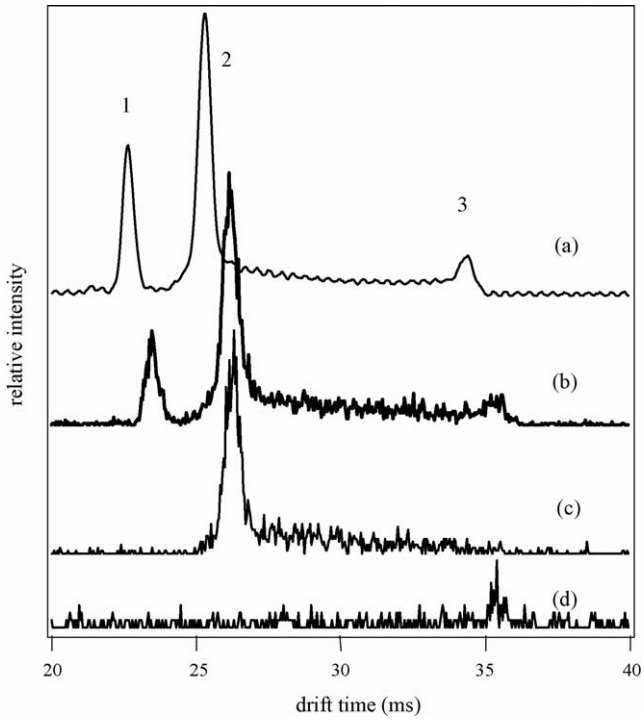

Fig. 1. Ion mobility spectra of DMP in air at 353 K containing 5 ppm_v of water vapor: (a) spectrum recorded at the ion mobility detector plate, (b) total ion current recorded at the mass spectrometer detector, (c) profile of m/z 108, $(DMP)H^+$, and (d) profile of m/z 215, $(DMP)_2H^+$. The peaks are identified as: 1, $(H_3O)_nH^+$; 2, $(DMP)H^+$; 3, $(DMP)_2H^+$.

$$-\frac{d[(DMP)_2H^+]}{dt} = k[(DMP)_2H^+] \quad (2)$$

The decomposition is occurring under low field conditions, i.e., $E/N < 2 \times 10^{-17}$ V cm^2, where E is the electric field and N is the number density of the drift gas [9]. Since the ion density is extremely low compared with that of the drift gas, the ions will be in thermal equilibrium with the drift gas and have a Boltzmann distribution of energies that is maintained at all times. The measurement of k over a well-defined temperature range then allows the determination of the activation energy E_a for the decomposition from the Arrhenius equation (Eq. (3)):

$$\ln k = \ln A - E_a/RT \quad (3)$$

Because there is no reverse activation energy for the dissociation, the measured activation energy E_a is the bond strength. Rate constants were determined from the mobility spectra, as detailed below.

Sufficient neutral base was introduced to the ion source so that the RIP just disappeared. The resulting mobility spectra for DMP at 353 K are shown in Fig. 2. With a 10 cm drift length (Fig. 2a), there is a broad maximum in peak intensity between the two sharp peaks for $(DMP)H^+$ and $(DMP)_2H^+$. This shows that some $(DMP)_2H^+$ is still being formed from $(DMP)H^+$ in the drift region beyond the first shutter and therefore some neutral

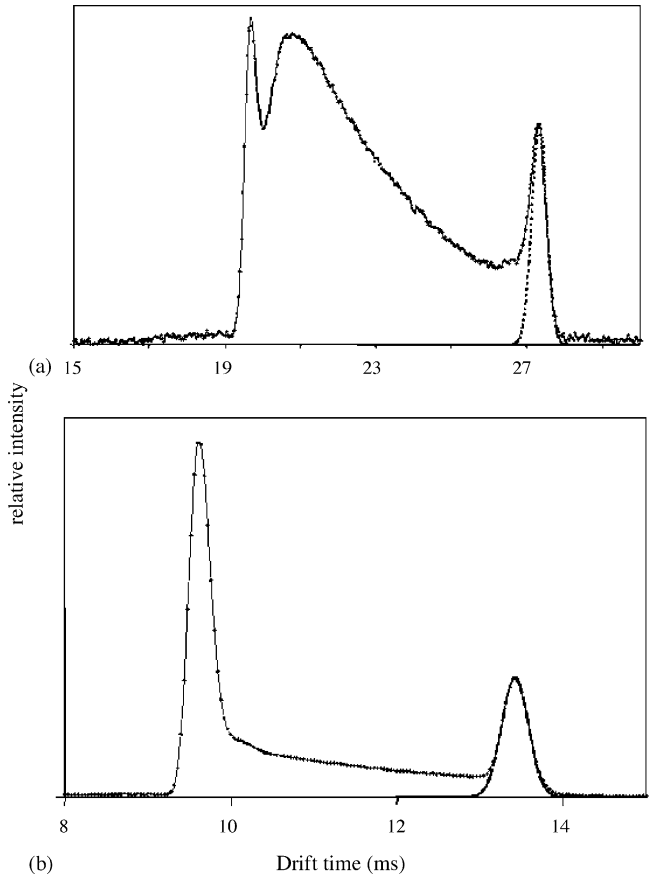

Fig. 2. Mobility spectra of DMP with: (a) 10.0 cm drift length and (b) 5.0 cm drift length: 353 K, 5 ppm_v water vapor. Gaussian functions fitted to the proton bound dimer peaks are shown.

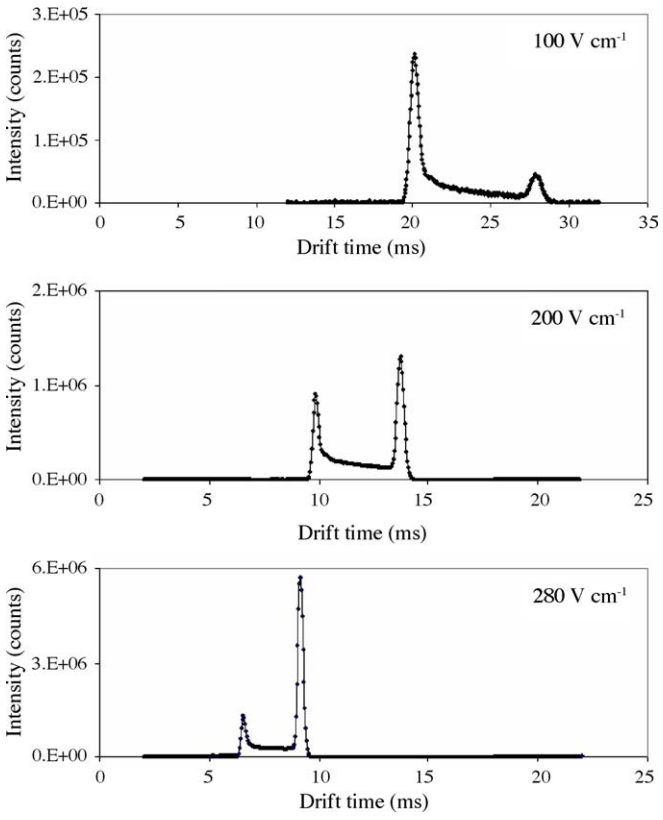

Fig. 3. Mobility spectra for DMP obtained with three different drift fields: 350.4 K, 5 ppm_v water vapor. The two peaks are those of the protonated molecule and the proton bound dimer.

DMP is passing into the drift region just beyond the shutter even though the flow of drift gas is in the opposite direction. This analysis is confirmed by the shape of the $(DMP)_2H^+$ peak. An isolated peak in a mobility spectrum should be almost Gaussian [10] but, as seen in the figure, although the trailing edge of the peak adheres closely to being Gaussian the leading edge does not. The extra width in this region is due to dimer ions formed just beyond the shutter which then survived transit to the detector plate. Only a small fraction of the lifetime of these ions is spent as $(DMP)H^+$, but it is sufficient to cause the broadening. When the drift distance is decreased to 5 cm by use of the second shutter the central broad maximum disappears (Fig. 2b) and the $(DMP)_2H^+$ peak becomes Gaussian. The penetration of neutral reagent in the 5 cm drift region, that is far removed from the sample inlet and exit, is therefore negligible and mobility spectra such as that in Fig. 2b present an opportunity for determining the rate constants for the decomposition of the proton bound dimer.

In the ion source where neutral reagent is present, $(DMP)H^+$ and $(DMP)_2H^+$ are in equilibrium with the neutral molecule (Eq. (4)):

$$(DMP)H^+ + DMP \rightleftharpoons (DMP)_2H^+ \quad (4)$$

When the ions enter the drift tube the concentration of DMP is decreased so that the equilibrium is disturbed and the concentration of $(DMP)_2H^+$ must decrease while that of $(DMP)H^+$ consequently increases. With no neutral present, only the reverse decomposition of $(DMP)_2H^+$ can occur, in a strictly first-order reaction described by Eq. (1). Under these conditions, the concentration of $(DMP)_2H^+$ ions that survive to the end of the drift region is proportional to the integrated intensity of the $(DMP)_2H^+$ peak. If the electric drift field strength is changed at constant temperature with a fixed drift length, the drift time and hence the time for dimer decomposition can be varied. The drift time t_d, measured at the dimer peak maximum, is given by Eq. (5), where L is the drift length, E the electric field strength, and the proportionality constant, K, is the mobility coefficient.

$$t_d = \left(\frac{L}{KE}\right) \quad (5)$$

A typical example of the effect of change of drift field strength on the spectrum of DMP is shown in Fig. 3. When the field is increased from 100 to 280 V cm^{-1}, the total ion intensity, the integral of the spectrum area, increases by a factor of 20. At the same time the relative intensity of $(DMP)_2H^+$ increases drastically and changes from being the lower of the peaks to being the higher. The lower intensity of the $(DMP)_2H^+$ peak relative to that of $(DMP)H^+$ at the low field strength is due to the dimer dissociation described by Eq. (1) and to a different time of observation. The change in total ion intensity may be attributable to two factors. The first is that the flux of ions arriving from the ion source at the shutter is proportional to the electric field strength, which is the same in both source and drift regions. When the field

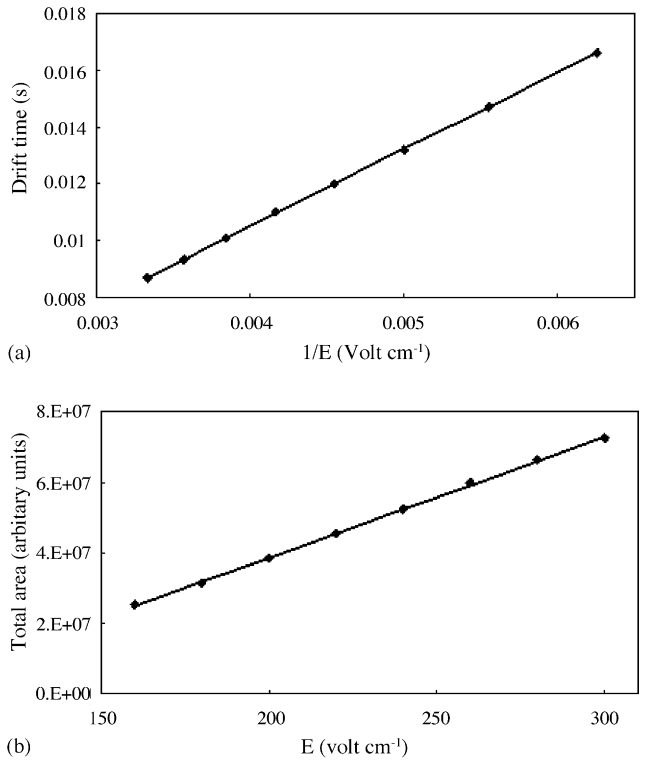

Fig. 4. (a) Correlation of $(DMP)_2H^+$ drift time with the reciprocal of electric field strength E and (b) correlation of total ion intensity (spectrum area) with the electric field strength E: 349.6 K, 5 ppm_v water vapor.

strength is decreased, the number of ions gated into the drift region during each 200 μs shutter open period decreases proportionately and hence the integrated intensity decreases. The second possible cause of decreased intensity is loss of ions to the drift tube walls by transverse diffusion; the longer the drift time of an ion cloud, the greater the loss.

The fractional ion loss in the drift region due to transverse diffusion is the same for all ions, independent of their individual mobilities, since when E/N is low the heavier dimer ions spend a longer time in the drift region than do the lighter more mobile monomer ions but their lower mobility exactly compensates for the longer time [11]. A measure of ion depletion due to transverse diffusion was obtained by comparing the integrated signal obtained at fixed drift field strengths for the 10 and 5 cm path lengths. There was a consistent difference, actually an increase, of 5% in the total ion signal obtained with the 5 cm compared with the 10 cm path. The increase may be attributed to slight physical and/or electrical differences between the two shutters. We presume that there is no or negligible loss of ion intensity due to transverse diffusion because the radius of the aperture grid (1.6 cm) in front of the larger detector plate is considerably bigger than the defining radius of the source (0.7 cm). Such an observation has been made previously [10] and is in agreement with diffusion theory [11]. The decrease of total ion intensity with decreasing field strength is wholly due to a decrease in the number of ions emanating from the source region.

The effect of drift field on the mobility spectrum of DMP at a temperature of 349.6 K is shown in Fig. 4. The dependence of the arrival time, t_d, of $(DMP)_2H^+$, measured at the peak maximum, on $1/E$ according to Eq. (5) is demonstrated in Fig. 4a. The equation of the linear correlation is $t_d = 2.7131E^{-1} - 0.0003$ with $R^2 = 0.9999$. The total ion intensity, measured by integrating ion intensity (area) over the whole spectrum, was always a linear function of electric field strength as illustrated in Fig. 4b. The linear correlation shown in the figure is described by the equation, integrated area $= 3.42E - 3 \times 10^7$ with $R^2 = 0.9995$. At lower field strengths than shown, the graph does depart from linearity with a smaller slope, and must tend towards the origin with decreasing field strength.

The method for determining the rate constant for dimer decay from the mobility spectrum involves interpreting the ion intensity between the peaks for $(DMP)H^+$ at t_m and for $(DMP)_2H^+$ at t_d. Ions that appear at drift times t, intermediate between t_m and t_d, were those that were gated into the drift region as $(DMP)_2H^+$ but arrived at the detector as $(DMP)H^+$, having dissociated at time t_x, where t_x is in the range from 0 to t_d. The value of t_x may be obtained from t, t_m and t_d.

If the drift speeds of monomer and dimer are v_m and v_d, respectively, and x is the distance from the shutter along the drift region at which dissociation occurred, then the distance traveled as dimer at speed v_d was x and as monomer at speed v_m was $L - x$, where L is the distance from shutter to detector. Since $v_m = L/t_m$ and $v_d = L/t_d$, then t is given by Eq. (6), which can be solved for the value of x given in Eq. (7). The time t_x at which the dimer decomposed at distance x from the shutter is then given by Eq. (8).

$$t = \frac{L - x}{v_m} + \frac{x}{v_d} = \frac{t_m(L - x)}{L} + \frac{t_d x}{L} \tag{6}$$

$$x = L\left(\frac{t - t_m}{t_d - t_m}\right) \tag{7}$$

$$t_x = \frac{x}{v_d} = t_d\left(\frac{t - t_m}{t_d - t_m}\right) \tag{8}$$

The ions decomposing at time t_x appear in the spectrum at time t and the integrated ion intensity after time t measures the dimer ions that have not decomposed at time t_x. Some of these ions will decompose before reaching the detector while others will not and constitute the dimer peak. The first-order decay of the dimer is then described by a graph of the logarithm of the non-decomposed dimer concentration (integrated intensity) at t_x versus t_x. Graphs for the decomposition of $(DMP)_2H^+$ at a constant temperature of 349.4 K and field strengths from 280 to 100 V cm^{-1} are shown in Fig. 5. The graphs start when $t_x = 0$, i.e., at $t = t_m$ and the initial sharp decrease in intensity on each curve denotes the move away from the monomer peak maximum. The precipitous fall at the end of each curve denotes the end of the dimer peak and of all ion intensity. The linear portions of the graphs, which increase in size as the drift times increase with decreasing field strength, are almost parallel, there being a slight decrease in slope of no more than 3% from the highest to the lowest field strength. The reason for this is not immediately obvious but could be due to a slight field-dependent inhomogeneity in the electric field. The small difference was

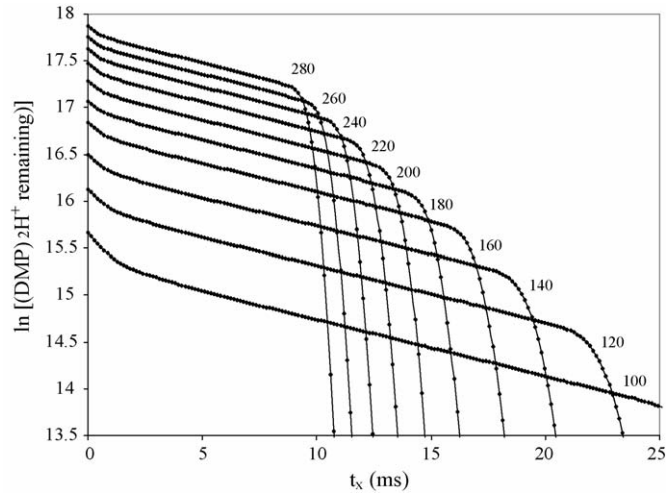

Fig. 5. Semi-logarithmic plots of $(DMP)_2H^+$ ion intensity remaining at time t_x (see Eq. (8)) at different field strengths E ($V\,cm^{-1}$): 349.4 K, 5 ppm_v water vapor.

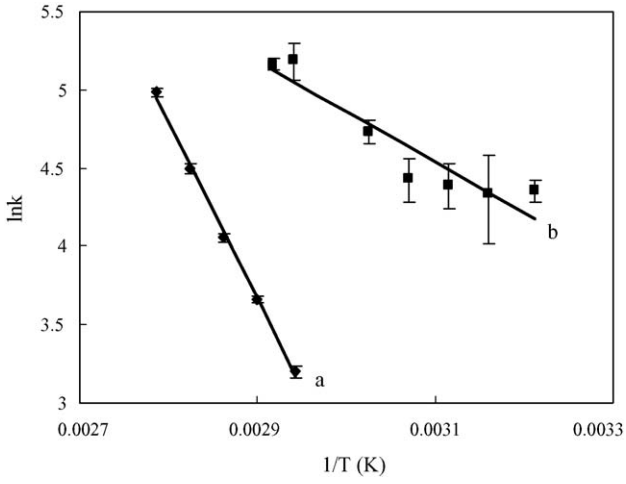

Fig. 6. Arrhenius plots for the dissociation of $(DMP)_2H^+$: (a) 5 ppm_v water vapor and (b) 2.0×10^3 ppm_v water vapor.

ignored and the rate constant k for the decay at the experimental temperature was obtained as an average of the negative of the slopes of all the graphs. The very narrow range of temperature, 340–360 K, over which the dissociation of $(DMP)_2H^+$ could be studied was determined by the very limited dynamic range of the mobility spectrometer. The results obtained at five temperatures in this range are shown in the Arrhenius plot of $\ln k$ versus $1/T$ (K) of Fig. 6, graph (a). The slope of the graph, which equals $-E_a/R$, yields an activation energy $E_a = 94 \pm 2\,kJ\,mol^{-1}$ at the 95% confidence level. The pre-exponential factor obtained from the intercept is $\log A\ (s^{-1}) = 15.9 \pm 0.4$. The results are shown in Table 1.

The above result for $(DMP)_2H^+$ was obtained with a water content of the drift gas of no more than 5 ppm_v. In order to investigate the effect of water on the dimer dissociation, a second set of experiments was performed in which the drift gas contained 2.0×10^3 ppm_v of water. The peak maximum of the dimer now occurred at a slightly longer drift time at each temperature and field strength. For example, at 340 K the drift time for a field of 220 $V\,cm^{-1}$ was 12.64 ms under dry conditions and 12.72 ms in the presence of added moisture. The range of temperature over which dissociation could be studied also changed, being 311–342 K compared with 338–358 K. The mobility spectra were processed in the manner described above to generate the Arrhenius plot shown in Fig. 6, graph (b) that yields $E_a = 31 \pm 5\,kJ\,mol^{-1}$ and $\log A\ (s^{-1}) = 6.3 \pm 1.4$. These results are shown in Table 1.

Experiments similar to those with DMP were carried out with DMMP. However, the temperature range required to observe dissociation was significantly higher than for DMP, being 478–498 K. Spectra were obtained under the very dry conditions of 5 ppm_v of water vapor, and with 5.0×10^2 and 2.0×10^3 ppm_v. The Arrhenius graphs obtained from the results are presented in Fig. 7 and the derived activation energies and pre-exponential factors are shown in Table 1. Unlike $(DMP)_2H^+$, a change in water vapor concentration had little effect on the dissociation of $(DMMP)_2H^+$.

The effect of water concentration on the rate constant for the dissociation of $(DMP)_2H^+$ was so pronounced that it was instructive to observe how water content affected the mobilities of $(H_2O)_nH^+$, and the protonated and proton bound dimers of both DMP and DMMP over a large temperature range. The results, also obtained with the 5.0 cm drift length and water vapor concentrations of 6, 5.0×10^2 and 2.0×10^3 ppm_v, are shown in Fig. 8 as graphs of the reduced mobilities, K_o versus temperature. The very limited range over which $(DMP)_2H^+$ was stable and could be investigated is immediately apparent.

Interestingly, attempts to measure the rate constants for the dissociation of the proton bound symmetrical dimers of some sterically hindered di- and tri-alkylamines in the mobility spectrometer at any temperature in its operating range were not successful. In fact, the dimers were not observable at all. This

Table 1
Kinetic and thermodynamic data for the reaction $M_2H^+ \rightarrow MH^+ + M$

M	Water (ppm_v)	E_a ($kJ\,mol^{-1}$)	$\log[A\ (s^{-1})]$	ΔH° [a] ($kJ\,mol^{-1}$)	k_+ [b] ($10^{-9}\,cm^3\,mol^{-1}\,s^{-1}$)
DMP	5	94 ± 2	15.9 ± 0.4	97	0.54
DMP	2×10^3	31 ± 5	6.3 ± 0.7	34	0.34
DMMP	5	127 ± 3	15.6 ± 0.3	131	4.24
DMMP	5×10^2	130 ± 2	15.3 ± 0.4	133	1.66
DMMP	2×10^3	115 ± 1	14.5 ± 0.3	119	0.34

[a] Obtained from $\Delta H^{\circ} = E_a + RT$.
[b] Calculated rate constant for the association reaction $MH^+ + M \rightarrow M_2H^+$.

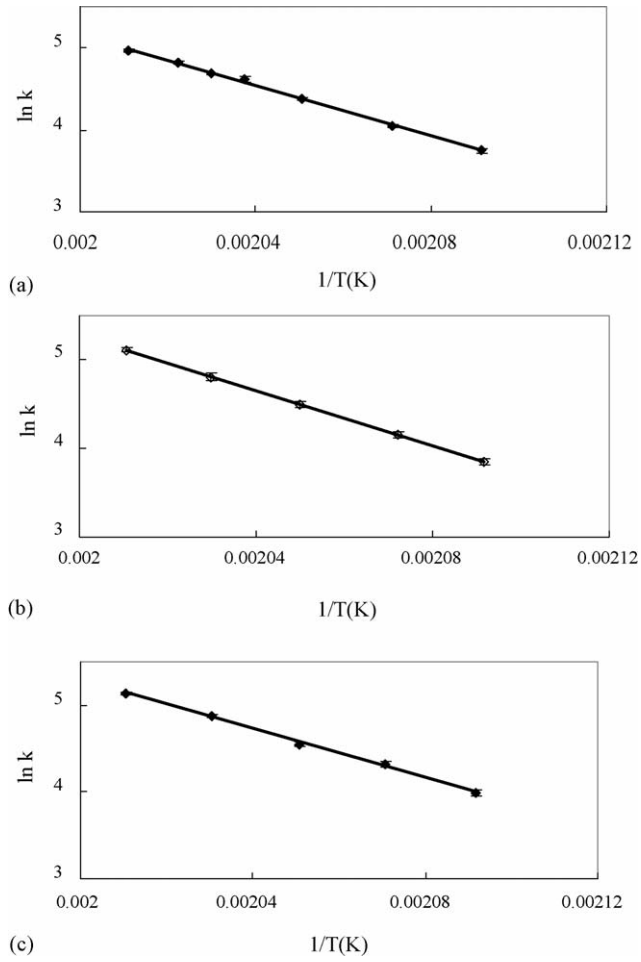

Fig. 7. (a) Arrhenius plots for the dissociation of $(DMMP)_2H^+$: (a) 5 ppm_v water vapor, (b) 5×10^2 ppm_v water vapor, and (c) 2.0×10^3 ppm_v water vapor.

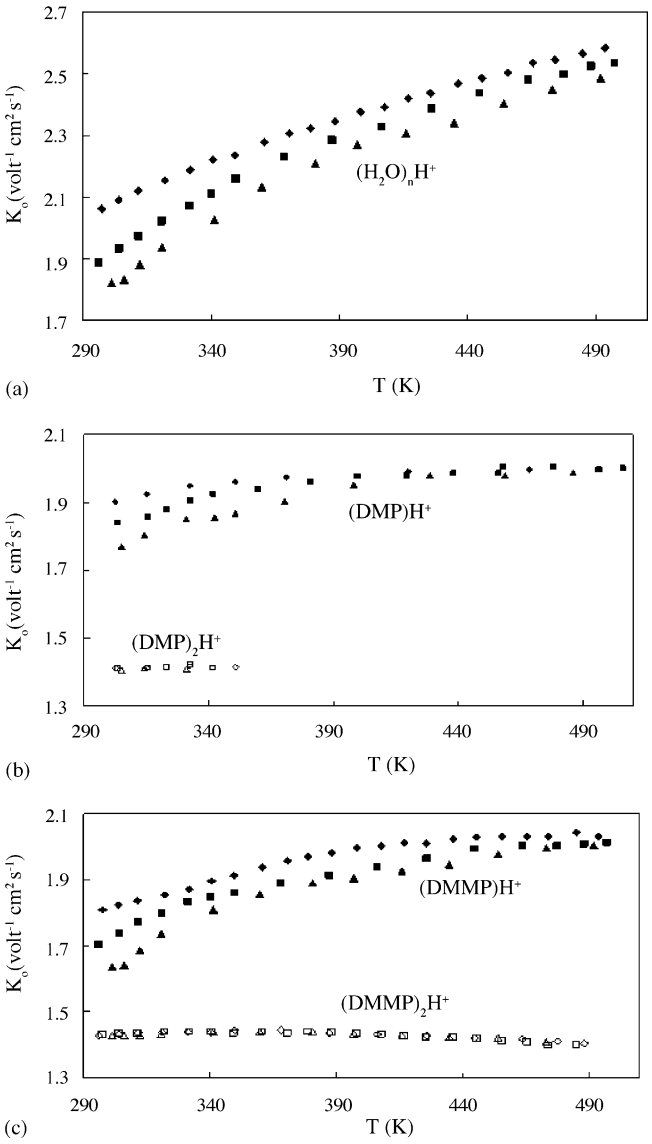

Fig. 8. Reduced mobilities as functions of temperature at different water vapor concentrations: (a) $(H_2O)_nH^+$, (b) $(DMP)H^+$ and $(DMP)_2H^+$, and (c) $(DMMP)H^+$ and $(DMMP)_2H^+$. Water vapor concentration: (♦, ◊) 6 ppm_v; (■, □) 5.0×10^2 ppm_v; (▲, △) 2.0×10^3 ppm_v.

was surprising since experiment has shown that the symmetrical proton bound dimers of these and other nitrogen bases have an almost constant hydrogen bond energy of 96 kJ mol^{-1} [12]. The lowest operating temperature of our instrument is slightly above room temperature. The required narrow temperature range was obviously sub-ambient. The very different behavior of these alkylamines compared with DMP must be associated with the very large negative entropies associated with their formation.

4. Discussion

The interpretation of the slope of the mobility spectrum between the monomer and dimer peaks gives a very simple method for determining the rate constant for the dissociation of the dimer. Since the ions entering the drift region are isolated from the neutral precursors and they are at extremely low density compared with the molecules of the drift gas, the results obtained are those for fully thermalized ions and the measured rate constants need no corrections for non-Boltzmann behavior. The pre-exponential factors are, with the exception of $(DMP)_2H^+$ in moist drift gas, of the order of 10^{15} s^{-1}, as expected for typical unimolecular dissociations [13].

Table 1 shows that there is a large difference in E_a of ~30 kJ mol^{-1} between the oxygen base DMMP and the nitrogen base $(DMP)_2H^+$. This difference is not unexpected since the activation energy for dimer dissociation is almost equal to the enthalpy for dissociation and the enthalpies of dissociation of symmetrical proton bound dimers of nitrogen bases are 30–35 kJ mol^{-1} less than those of oxygen bases [14]. This latter information has been provided mainly by PHPMS. Unfortunately, no experiments have been performed with DMP or DMMP but comparison may be made with results for similar compounds. In an early paper, Yamdagni and Kebarle showed that for symmetrical proton bound dimers of several nitrogen bases the enthalpy of association was constant at close to −96 kJ mol^{-1} [12]. For the proton bound dimer of 2,6-dimethylpyridine, Meot-Ner and Sieck obtained by PHPMS an enthalpy of association of -97.5 ± 2.1 kJ mol^{-1} and essentially

the same value, $-96.2 \pm 2\,\mathrm{kJ\,mol^{-1}}$, for 2-methylpyridine [15]. A similar value would be expected for DMP.

The enthalpy change for the dissociation of a proton bound dimer, the negative of that for association, may be obtained from the activation energy for dissociation if the very reasonable and usual assumption is made that there is no reverse activation energy. The activation energy is related to the standard reaction enthalpy by Eq. (9).

$$\Delta H^\circ = E_a + RT \tag{9}$$

ΔH° in this equation is temperature dependent so the values calculated from the measured activation energies and shown in Table 1 are for the temperature at the mid-range of each experiment. The value of $97 \pm 2\,\mathrm{kJ\,mol^{-1}}$ obtained for $(DMP)_2H^+$ in the presence of 5 ppm_v of water is identical with the value obtained by Meot-Ner and Sieck for the mono- and dimethyl pyridine isomers.

The proton bound dimer of DMMP decomposes in a first-order process at a much higher temperature than does that of DMP, consistent with its higher bond energy as an oxygen rather than a nitrogen base. Larson and McMahon [3] and Meot-Ner [16] have shown that the dissociation enthalpy of many symmetrical proton bound oxygen bases is approximately $133\,\mathrm{kJ\,mol^{-1}}$. This value is essentially the same as that in Table 1 for DMMP in the presence of 5 ppm_v of water. The equality of the measured enthalpies with those derived from our kinetic experiments validates the activation energies derived from the observation of the decay of proton bound dimers in a drift tube operating at atmospheric pressure with low moisture content.

The rate constants obtained for the dissociations allow calculation of the related forward rate constants for association. The rate constant k_- for the dissociation of a proton bound dimer M_2H^+ is related to the rate constant k_+ for the association reaction (Eq. (10)) by Eq. (11), where K is the equilibrium constant and c° is the standard concentration of 1 atm.

$$MH^+ + M \leftrightharpoons M_2H^+ \tag{10}$$

$$K = \exp\left(\frac{-\Delta G^\circ}{RT}\right) = \exp\left(\frac{-\Delta H^\circ}{RT} + \frac{\Delta S^\circ}{R}\right) = \frac{k_+ c^\circ}{k_-} \tag{11}$$

The value of k_+ for DMP and DMMP may be obtained if a value of ΔS° for the association reaction can be estimated. For most such association reactions ΔS° lies in the range -100 to $-125\,\mathrm{J\,K^{-1}\,mol^{-1}}$. Examples for nitrogen bases are: methylamine, $-99\,\mathrm{J\,K^{-1}\,mol^{-1}}$ [14]; pyridine, $-124\,\mathrm{J\,K^{-1}\,mol^{-1}}$ [17]; pyridine and 2-methylpyridine, $-117\,\mathrm{J\,K^{-1}\,mol^{-1}}$ [15]. Examples for oxygen bases are: water, $-100\,\mathrm{J\,K^{-1}\,mol^{-1}}$ [18], $-102\,\mathrm{cal\,K^{-1}\,mol^{-1}}$ [19] and acetone, $-100\,\mathrm{cal\,K^{-1}\,mol^{-1}}$ [20]. Taking a value of $-120\,\mathrm{J\,K^{-1}\,mol^{-1}}$ for the formation of $(DMP)_2H^+$ and a value of $-100\,\mathrm{J\,K^{-1}\,mol^{-1}}$ for $(DMMP)_2H^+$, the value of k_+ was calculated using Eq. (11) for each of the experiments at the mid-point of the temperature range. The results, presented in the last column of Table 1, although somewhat scattered, are all of the order of $10^{-9}\,\mathrm{cm^3\,mol^{-1}\,s^{-1}}$. The value of the capture rate constant calculated from the variational/classical trajectory theory [21] with $\alpha = 1.24 \times 10^{-24}\,\mathrm{cm^3}$ and $\mu = 2.24\,\mathrm{D}$ for DMP is $1.8 \times 10^{-9}\,\mathrm{mol^{-1}\,cm^3\,s^{-1}}$ for the formation of $(DMP)_2H^+$. Similarly, with $\alpha = 9.9 \times 10^{-24}\,\mathrm{cm^3}$ and $\mu = 2.86\,\mathrm{D}$ for DMMP, the capture rate constant is $1.7 \times 10^{-9}\,\mathrm{mol^{-1}\,cm^3\,s^{-1}}$ for the formation of $(DMMP)_2H^+$. All the association reactions are occurring at or close to the capture rate as expected for an association reaction occurring at atmospheric pressure when very efficient collisional stabilization of the hyperenergetic initial ion–molecule complex should occur.

5. The effect of water vapor concentration

Table 1 shows that increased water content of the drift gas has, within experimental uncertainty, little effect on the decomposition of $(DMMP)_2H^+$. However, the Arrhenius parameters for the decomposition of $(DMP)_2H^+$ are markedly changed, both the pre-exponential factor and the activation energy being considerably reduced. Over the range of temperature that decomposition is observable, reaction occurs at a greater rate for this dimer under very moist conditions. A possible clue to an explanation for this phenomenon is shown in Fig. 8 where reduced mobility at different moisture levels of drift gas is plotted against temperature for $(H_2O)_nH^+$ and the monomers and dimers of DMP and DMMP.

When the mass and/or volume of an ion are increased, all other things being equal, its mobility in the low field limit will decrease. This is described by the formula for the mobility, Eq. (12), in which q is the electronic charge, N the molecular number density, μ the reduced mass of the ion and neutral drift gas molecule, $\Omega_D(T)$ an average ion-neutral collision cross section, T the absolute temperature and α is a small correction factor with a value very close to unity [9].

$$K = \frac{3}{16}\frac{q}{N}\left(\frac{2\pi}{\mu kT}\right)^{1/2}\frac{1+\alpha}{\Omega_D(T)} \tag{12}$$

The reduced mobility K_o is defined by Eq. (13), where 273 K and 760 Torr are standard temperature and pressure.

$$K_o = K\left(\frac{273}{T}\right)\left(\frac{P}{760}\right) \tag{13}$$

If the potential between ion and drift gas molecule is determined mainly by an ion-induced dipole interaction that varies with distance as r^{-4} then Ω_D varies as $T^{-1/2}$ and since N is proportional to $1/T$ then K_o is invariant with temperature [11]. This will hold true provided that the nature of the ion does not change. Fig. 8 shows that the K_o values for the dimers of both DMP and DMMP remain almost constant over the experimental temperature ranges and are also independent of very large changes in the water content of the drift gas. We noted earlier that the drift time of $(DMP)_2H^+$ increased by less than 1% when the water concentration was changed by a factor of 200. The same small change was observed for $(DMMP)_2H^+$. By contrast, the K_o values of the RIP and of the monomers show significant changes in some or all of the temperature ranges. We attribute this difference to the effect of temperature on the varying levels

Table 2
Calculated average molar masses of hydrated ions at different water concentrations and temperatures

Core ion	H_2O (ppm_v)	298 K	340 K	488 K
H_3O^+	5	78	62	39
	400	100	80	52
	2500	113	92	56
$(DMP)H^+$	5	109	108	108
	400	121	111	108
	2500	125	117	108
$(DMMP)H^+$	5	134	125	125
	400	143	134	125
	2500	143	141	125

of clustering of water molecules around the core ions of the RIP and monomer ions and the lack of significant hydration of the dimers. There was for each dimer, over the very narrow experimental temperature range of the kinetic experiments, an increase in K_o of less than 1% from 5 to 2000 ppm_v water content.

The effect of clustering on reduced mobility is evident at all temperature for $(H_2O)_nH^+$, the higher the water concentration the lower the value of K_o; the greatest reduction is observed at the lowest temperatures and the least at the highest temperatures. An ion in equilibrium with solvating molecules has a drift time determined by the sum of the times spent as each solvate. Available thermodynamic data allows an estimate of the extent of the degree of clustering of water molecules around the proton at any temperature and the number average ion mass [14]. The calculated average masses at equilibrium at the three experimental water concentrations and temperatures of 298, 340, and 488 K are shown in Table 2. The changes in reduced mobilities shown in Fig. 8 with change of both temperature and water concentration reflect these different degrees of hydration of the proton, the smaller the average ion mass the higher the mobility. In particular, there is a significant difference in mobility with water concentration, even at the highest temperature.

In contrast to the hydrated proton, the K_o values of both monomers are affected by water concentration at low temperatures but at high temperature, above 420 K for $(DMP)H^+$ and above 500 K for $(DMMP)H^+$, the values tend to be independent of concentration and approaching a constant value. Below these temperatures, K_o decreases with decreasing temperature and at any temperature is lower the higher the water concentration. There is no data in the literature for the enthalpy of hydration of either $(DMP)H^+$ or $(DMMP)H^+$ but estimates may be made by reference to analogous ions. For $(DMP)H^+$, data for the association of the ion with one molecule of water may be obtained by reference to the data of Meot-Ner and Sieck for the monohydration of alkyl-substituted pyridines [15]. For 2,6-dimethyl-, 2-*i*-propyl-, and 2-*t*-butyl-pyridines, the respective standard enthalpies ($kJ\,mol^{-1}$) and entropies ($J\,K^{-1}\,mol^{-1}$) are: −55.2 and −108; −59.4 and −121; and −59.4 and −129. The results in Table 2 for DMP were calculated with estimated values of $-55.2\,kJ\,mol^{-1}$ and $-110\,J\,K^{-1}\,mol^{-1}$. For $(DMMP)H^+$, we estimate the enthalpy of association of one water molecule from the correlation obtained for the hydrogen bond in monohydrated oxonium ions, $–O–H^+\cdots OH_2$, of $-\Delta H^\circ\ (kJ\,mol^{-1}) = 127 - 0.30\Delta(PA)$, where $\Delta(PA)$ is the difference in proton affinity between the two ligands [16]. The proton affinity of DMMP is $902\,kJ\,mol^{-1}$ [22], $230\,kJ\,mol^{-1}$ higher than that of water. The hydration enthalpy is then $-58\,kJ\,mol^{-1}$ and a typical hydration entropy value for such a reaction is $-100\,J\,K^{-1}\,mol^{-1}$ [14]. The calculated average molar masses of the hydrates of $(DMP)H^+$ and $(DMMP)H^+$ will be minimal values since the formation of higher hydrates, for which thermodynamic information is not available, is not taken into account. $(DMP)H^+$ (108 Da) is only slightly hydrated with 5 ppm_v of water at any temperature but tends towards the mass of the hydrate (126 Da) with 400 and 2500 ppm_v at 298 K and to a lesser extent at 340 K. $(DMMP)H^+$ (126 Da) is highly hydrated at all water concentrations at 298 K but is not hydrated at 525 K. These calculations are in approximate agreement with the picture presented by the reduced mobilities of Fig. 8. The values for $(DMP)H^+$ become constant and invariant with temperature above 420 K at any water concentration. The values for $(DMMP)H^+$ are showing the same tendency at much higher temperature.

The decomposition kinetics of $(DMP)_2H^+$ were obtained in the range 340–360 K where the ions are bare at low water concentration but become hydrated at higher concentration. By contrast, the decomposition kinetics of $(DMMP)_2H^+$ were obtained in the range 478–497 K where ion hydration is minimal. A change of water concentration had no effect on the measured rate constant for the dissociation of $(DMMP)_2H^+$ but had a profound effect on the dissociation of $(DMP)_2H^+$. This suggests that water is enhancing the decomposition of $(DMP)_2H^+$ by changing the mechanism.

The most probable reason for the lower activation energy with high water concentration is that decomposition is now by a switching mechanism with one or more water molecules displacing DMP (Eq. (14)).

$$(DMP)_2H^+ + H_2O \rightarrow (DMP)H^+(H_2O) + DMP \qquad (14)$$

Although water does not add to the dimer to an extent that affects the reduced mobility, an encounter could be sufficient to sometimes initiate reaction. Since there is no DMP in the drift gas, the energetically favored reverse reaction cannot occur. The enthalpy change for Eq. (14) is the difference between the solvating power of DMP and H_2O. With the experimental $-97\,kJ\,mol^{-1}$ for DMP and the estimated $-55\,kJ\,mol^{-1}$ for H_2O, the expected enthalpy change and activation energy for Eq. (14) is $42\,kJ\,mol^{-1}$, which is in reasonable accord with the experimental $34\,kJ\,mol^{-1}$. The decomposition of $(DMMP)_2H^+$ is essentially unaffected by water, maybe because at the higher temperature the lifetime of the hydrate is too short for the necessary rearrangement or maybe because if short-lived water attachment occurs, it is through hydrogen bonding to an oxygen that is not participating in the $O–H^+\cdots O$ linkage.

6. Conclusions

An ion mobility spectrometer has been used to obtain the rate constants for the thermal decomposition of the proton bound

dimers of DMP and DMMP. The reaction time was changed by varying the electric drift field strength and hence changing the drift time. The rate constants have been determined from a calculation of the number of dimer ions remaining at any time in their passage through the drift region. Even though the temperature range over which the experiments can be carried out is very limited, being only of the order of 20 K, the precision of the method is excellent. The reaction enthalpies calculated from the activation energies are in excellent agreement with those from published PHPMS equilibrium studies. The results obtained for $(DMMP)_2H^+$ were unaffected by a factor of 400 change in water content of the drift gas but both the activation energy and the pre-exponential factor for the decomposition of $(DMP)_2H^+$ were considerably reduced when the water concentration was increased. This is attributed to a displacement reaction with a lower activation energy (Eq. (14)) replacing the unimolecular decomposition reaction.

The reduced mobilities of $(DMP)_2H^+$ and $(DMMP)_2H^+$ show little change with more than a 400-fold increase in water concentration whereas those of $(DMP)H^+$ and $(DMMP)H^+$ show a large change at low temperatures. Of course the dimers are relatively large entities and the addition of one water molecule, for example, would not change the reduced mass or volume to as great an extent as it would for a monomer. Nevertheless, the invariance with water concentration implies that the dimers are not hydrated to any significant extent at any temperature whereas the monomers are. Under the experimental conditions of very low water concentration and the chosen temperature range for each dimer, hydration does not interfere with the unimolecular decomposition reaction of interest.

Although the temperature range for observation of dimer decomposition is only 20 K, the high precision of the experiment provides a simple method for obtaining Arrhenius parameters. The high pressure ensures that the ions always have a Boltzmann distribution of energies and so no corrections are required. The method could be applied to other systems of symmetrical dimers and with the upper temperature limit of the present apparatus activation energies up to $\sim$150 kJ mol^{-1} could be determined. For asymmetric dimers, a dual shutter instrument with sufficient distance between source and first shutter would be required to isolate the dimer of interest from the accompanying symmetrical dimers.

Acknowledgements

The financial support from NASA (grant no. NAGY-4558) and US Army Research Office (grant no. DAAH04-95-1-0541) is gratefully acknowledged. The authors wish to recognize the contributions of Jose Sterling for his help with data collection. The authors also wish to recognize the contributions by their late U.S. Army Edgewood Chemical Biological Center, Aberdeen Proving Ground colleague and friend, Donald B. Shoff, 12 July 1956–20 October 2002. He is greatly missed.

References

[1] P. Kebarle, in: J.M. Farrar, W.H. Saunders (Eds.), Techniques of Chemistry, vol. XX, Wiley-Interscience, New York, 1988, p. 221.
[2] R.G. Keesee, A.W. Castleman, J. Phys. Chem. Ref. Data 15 (1986) 1011.
[3] J.W. Larson, T.B. McMahon, J. Am. Chem. Soc. 104 (1982) 6255.
[4] P. Kebarle, Int. J. Mass Spectrom. 200 (2000) 313.
[5] P.B. Armentrout, Top. Organomet. Chem. 4 (1999) 1.
[6] R.G. Cooks, J.T. Koskinen, P.D. Thomas, J. Mass Spectrom. 34 (1999) 85.
[7] J.L. Holmes, C. Aubry, P.M. Mayer, J. Phys. Chem. 103 (1999) 705.
[8] R.G. Ewing, G.A. Eiceman, J.A. Stone, Int. J. Mass Spectrom. 193 (1999) 57.
[9] E.A. Mason, E.W. McDaniel, Transport Properties of Ions in Gases, Wiley-Interscience, New York, 1988.
[10] G.E. Spangler, M.J. Cohen, in: T.W. Carr (Ed.), Plasma Cromatography, Plenum Press, New York, 1984, p. 1.
[11] E.A. Mason, in: T.W. Carr (Ed.), Plasma Cromatography, Plenum Press, New York, 1984, p. 43.
[12] R. Yamdagni, P. Kebarle, J. Am. Chem. Soc. 95 (1973) 3504.
[13] I.N. Levine, Physical Chemistry, third ed., McGraw-Hill, New York, 1988.
[14] P.J. Linstrzm, W.G. Mallard (Eds.), NIST Chemistry WebBook, NIST Standard Reference Database Number 69.
[15] M. Meot-Ner, L.W. Sieck, J. Am. Chem. Soc. 105 (1983) 2956.
[16] M. Meot-Ner, J. Am. Chem. Soc. 106 (1984) 1257.
[17] M. Rusyniak, Y. Ibrahim, E. Alsharaeh, M. Meot-Ner, M.S. El-Shall, J. Phys. Chem. A 107 (2003) 7656.
[18] M. Meot-Ner, C.V. Speller, J. Phys. Chem. 90 (1986) 6616.
[19] A.J. Cunningham, J.D. Payzant, P. Kebarle, J. Am. Chem. Soc. 94 (1972) 7627.
[20] M. Meot-Ner, S. Scheiner, W.O. Yu, J. Am. Chem. Soc. 120 (1998) 6980.
[21] T. Su, W.J. Chesnavich, J. Chem. Phys. 76 (1982) 5183.
[22] M. Tabrizchi, S. Shooshtari, J. Chem. Thermo. 35 (2003) 863.